Characterization of Polyacrylic Acid Modified Zinc Phosphate Crystal Conversion Coatings

J. L. WRAGG,[1] J. E. CHAMBERLAIN,[1] L. CHANN,[1] H. W. WHITE,[1,*] T. SUGAMA,[2] and S. MANALIS[3]

[1]Department of Physics and Astronomy, University of Missouri, Columbia, Missouri 65211; [2]Energy Efficiency and Conservation Division, Department of Applied Science, Brookhaven National Laboratory, Upton, New York 11973; and [3]Digital Instruments, Inc., 6780 Cortona Drive, Santa Barbara, California 93117

SYNOPSIS

Raman spectroscopy and atomic force microscopy have been used to investigate the composition and surface structure of polyacrylic acid modified zinc phosphate crystal conversion coatings on steel. Zinc phosphate coatings are used extensively to provide corrosion protection and to improve adherence of topcoatings to steel. Within the last few years it has been demonstrated that addition of high molecular weight polyacrylic acid (PAA) to the phosphating bath can significantly improve both resistance to corrosion and topcoat adherence. It has been reported that the addition of PAA reduces the size of crystallites, which leads to greater film ductility, and therefore to fewer sites for corrosive attack, and that organic molecular segments from the PAA are incorporated into the surface structure and provide additional adhesive bonding with polymeric topcoats. In this work Raman spectra show the compositions of both unmodified and PAA modified films to be zinc phosphate dihydrate, $Zn_3(PO_4)_2 \cdot 2H_2O$. Atomic force microscopy (AFM) was used to measure the morphologies of single crystallite surfaces. Morphologies of the unmodified and modified films obtained by AFM are in general quite similar, but subtle differences are apparent.

INTRODUCTION

Crystalline Zinc Phosphate Films

Crystalline zinc phosphate films have been used extensively for many years to protect cold-rolled and mild carbon steel against corrosion and to provide a good substrate for paint adhesion. Films are grown in a phosphoric acid bath containing zinc phosphate at elevated temperatures. Films used for corrosion protection on commercial products are composed of a dense, microstructural array of interlocking crystallites, some tens of microns in lateral dimensions, yielding a film 50–100 microns in thickness. Corrosion protection is good, especially if the surface is completely covered. Recipes can be tailored to obtain reproducible films with complete coverage on various steels, but a given recipe may not always give good protection for all steels. High-quality films with good coverage are more easily attained for low carbon steels than for those with high carbon content. Difficulties obtaining uniform coverages have been noted for some low-grade reclaimed (mixed) steels.

Several efforts to characterize zinc phosphate films have been reported. Ghali and Potvin[1] explored the mechanisms associated with different steps during film growth. They measured the relative abundance of iron and zinc in the films and noted that the iron content dropped dramatically with time of growth. They and earlier workers concluded the outer film to be trizinc orthophosphate tetrahydrate (hopeite), $Zn_3(PO_4)_2 \cdot 4H_2O$. More recently, Sugama et al.[2,3] used a number of surface analytical techniques to further investigate mechanisms of film growth and structure. A three-layer structure was proposed, with the outermost layer being zinc phosphate dihydrate, $Zn_3(PO_4)_2 \cdot 2H_2O$.

* To whom correspondence should be addressed.

Journal of Applied Polymer Science, Vol. 50, 917–928 (1993)
 CCC 0021-8995/93/050917-12

Polyacrylic Acid (PAA)-Modified Zinc Phosphate Films

In an effort to improve the corrosion protection capabilities of zinc phosphate coatings, Sugama et al.[2,3] grew films with selected high-molecular-weight organic acids added to the phosphating bath. Ordinary phosphate films are subject to cracking, which provides sites for corrosive attack. They conjectured that segmented organic acid groups in the bath might provide additional nucleation sites for crystallite growth, thereby leading to a film with smaller crystallites and greater strength during flexure. The decreasing crystal size, they believe, is due primarily to segmental chemisorption to the precipitated crystal surfaces of functional electrolyte groups such as carboxylic acid ($-COOH$) and sulfonic acid ($-SO_3H$). The PAA molecule has a polyelectrolyte character. Its structure is, $[-CH_2CH(COOH)-]_n$, and can be considered as consisting of a hydrophobic main chain $(-CH_2-CH-)_n$, and hydrophilic carboxylic acid pendent groups (COOH).

Sugama et al.[2,3] used ESCA to identify elements at the outermost surface sites of PAA-modified films. The results suggested that certain areas of the film surface were covered with a thin PAA layer no thicker than 5 nm. Further analysis of binding energy shifts for C=O and COOH indicated the outermost surface contained organic functional species such as ionic carboxylate and carboxylic acid groups.

Sugama et al.[2,3] found that mechanical properties, corrosion protection, and adhesion to polymeric topcoats was significantly improved by the addition to the solution bath of a few percent by weight of PAA with a molecular weight in the neighborhood of 50,000. These improved properties are related to the thickness and fineness of the zinc phosphate crystallites. Film characteristics are usually optimum for PAA concentrations of 2–3% in the solution bath.

Improved Mechanical Properties

Using flexural stress–strain measurements Sugama and co-workers[3] demonstrated that the addition of 2–3% PAA to the solution bath improved the resultant flexural modulus by a factor of two over control specimens without PAA. The flexural stress associated with the yield point was increased by a factor of 1.7. The relative toughness of the PAA-modified film was also increased significantly.

Improved Corrosion Resistance Properties

Comparisons by Sugama[4] of DC electrochemical polarization curves in a 25°C deaerated 0.5*M* NaCl solution for specimens of untreated steel, steel with an unmodified zinc phosphate coating, and steel with a zinc phosphate coating modified with 2–4% PAA in the phosphating bath demonstrated two important results. First, compared with untreated steel, steel with an unmodified zinc phosphate coating had a significantly lower corrosion current, and the corrosion potential was moved to less negative values. Second, a PAA-modified zinc phosphate coating further enhanced the corrosion resistance of the zinc phosphate film.

Improved Adhesion Properties

Performance evaluation revealed that paint adhesion is markedly better, up to a factor of ten, for films grown in baths containing PAA. It is conjectured that organic functional species from the PAA remain on the surface and form a base for adhesion of polymeric topcoats. The organic surface groups would act as a primer. Peel tests indicated topcoat adhesion was increased dramatically, by a factor or ten or more, for optimum PAA levels. Following exposure to aggressive media (hot H_2SO_4) solution at 80°C for 30 days) the mode of adhesive failure was cohesive in the zinc phosphate precoat. Evidently, organic functional species present at the precoat–topcoat interfacial region were instrumental in giving a measure of protection to the adhesive bonds. The location of failure within the zinc phosphate precoat suggests that it will be necessary to strengthen the precoat to further improved adhesive performance.

The improvement in adhesion performance has been sufficient to allow commercial application of polymeric topcoats by electrostatic precipitation rather than by conventional spraying, thereby greatly reducing adverse environmental impacts during application. The overall cost savings associated with the application of polymeric topcoats may rival or eclipse cost savings due to improved corrosion performance.

Goals of Current Studies

The goals of this work were to characterize and compare surface properties of unmodified zinc phosphate films and zinc phosphate films modified with PAA using Raman spectroscopy and atomic

force microscopy (AFM). In particular, evidence for the presence of PAA or organic functional species from the PAA in the modified films was sought.

EXPERIMENTAL

Film Preparation

Unmodified and PAA-modified crystalline zinc phosphate films were grown following recipes as reported by Sugama et al.[2,3] PAA content in the solution bath ranged from 0 to 5% by weight. For example, a 1.0 wt % PAA film would be prepared as follows: The steel sample was first wiped with acetone-soaked tissues to remove any surface contamination due to mill oil. The steel was then immersed for up to 15 min in the conversion solution consisting of 5 g zinc phosphate ($Zn_3(PO_4)_2 \cdot 2H_2O$), 10 g (85% H_3PO_4 solution), 360 g water, and 16 g (25% PAA) at a temperature of 90°C. After immersion, the surface was rinsed with water, and then dried in an oven at 150°C for 15 min to remove any moisture from the deposited conversion film surface and to solidify the PAA macromolecules.

The high-strength steel substrates were obtained from Bethlehem Steel Corp. The PAA, molecular weight of 50,000, was obtained from Aldrich Chemical Co. The zinc phosphate dihydrate was obtained from Alfa Products. Numerous unmodified and modified films were grown under a variety of conditions. Results from films with 0, 1, 2, and 5% PAA in the solution bath are presented here. Results were essentially unchanged over the concentration range from 1 to 5%. Some films were baked at various elevated temperatures up to 150°C, and others left unbaked to determine the effect of baking on surface properties.

For both modified and unmodified films the zinc phosphate crystallites were long and rectangularly shaped, with significant variation in size. On films grown with PAA in the solution bath many of the crystallites on the surface were 5–10 μm wide by 10–50 μm long. The dimensions of crystallites grown without PAA in the bath were roughly twice these values.

Raman and Micro-Raman Spectroscopy

Raman and micro-Raman spectra were taken with a laboratory assembled spectrometer that employs an argon ion laser, a spectrograph, and a cooled CCD detector. The 514.5-nm laser line was used for all measurements. The Raman spectra were taken on surface areas of approximately 1 mm.^{2} The micro-Raman attachment was a modified optical microscope that provided a spot size approaching one micron in diameter. The spot could be placed on an individual crystallite or other surface feature and a spectrum measured. Raman spectra could be obtained in a few minutes or less with laser powers typically less than 200 mW, so no surface damage or modification was expected.

Atomic Force Microscopy

Digital Instruments, Inc. Nanoscope II contact-type AFM and Nanoscope III contact-type and tapping mode AFM instruments were used to obtain images on unmodified and modified films. The tips are located on the end of a thin triangular shaped cantilever that has an Au reflective coating. SiN tips were used in this work for contact AFM on the Nanoscope II, and etched silicon tips for *both* the contact and the tapping mode AFM on the Nanoscope III. The SiN tips used on the Nanoscope II have a larger end radius than the etched silicon tips used on the Nanoscope III. For both contact and tapping AFM the position of the tip is sensed optically; however, for tapping AFM the tip is also vibrated and held just above the surface. The sample surface is detected by oscillating the cantilever at or near its natural frequency and then approaching the surface with the tip until the tip taps lightly on the surface. This tapping mode AFM eliminates the lateral force between the tip and sample and is particularly useful for obtaining images of soft and deformable surfaces.

Imaging with STM was attempted but the tunneling current generated was not sufficient to obtain images.

AFM scans were made on individual zinc phosphate dihydrate crystallites. Images up to 5,000 nm on a side were obtained. For several very smooth regions good quality scans could be obtained on areas down to 100 × 100 nm, but most often the minimum size for quality scans was on the order of 300 × 300 nm. Atomic resolution could not be obtained on any of the crystallites examined.

RESULTS AND DISCUSSION

Raman and Micro-Raman Spectroscopy

The Raman spectra of the surface and the micro-Raman spectra of individual crystallites demonstrate clearly that the surface film is composed,

overwhelmingly, of crystallites of zinc phosphate dihydrate, $Zn_3(PO_4)_2 \cdot 2H_2O$. A systematic study in our laboratory of the series $Na_{3-m}H_mPO_4 \cdot nH_2O$ (m = 0, 1, 2 and n = 1, 7, and 12), and a similar potassium phosphate series, has demonstrated that the Raman signature in the 300–1200 cm^{-1} range is highly sensitive to the chemistry of the phosphate and that the 3000–3600 cm^{-1} region is a sensitive and powerful indicator of the number of waters of hydration in metal phosphate crystals. These two regions in the Raman spectra were useful for identifying the crystallites. The region from roughly 300 to 1200 cm^{-1} showed several peaks that could be associated with zinc phosphate dihydrate. No evidence for zinc phosphate tetrahydrate, $Zn_3(PO_4)_2 \cdot 4H_2O$, in either spectral range was found. Identification was made by comparing Raman spectra from the films with Raman spectra taken on zinc phosphate dihydrate and other metal phosphates with different numbers of waters of hydration. Peaks due to the O—H stretching mode for hydroxyls and molecular water appear in the spectral region from 3000 to 3600 cm^{-1}. This spectral window was used to confirm that the zinc phosphate films were the dihydrate form, although there was ample evidence of this in the other spectral window. For these samples the regular Raman technique (i.e., not micro-Raman) probes the entire depth of the surface deposits of zinc phosphate. These crystals are sufficiently optically transparent that the incident laser beam readily reaches the entire crystal, and the Raman scattered light easily escapes to be detected. The similarity of all Raman spectra, for both the regular and micro-Raman techniques, indicates that there is no substantial layer of any other phosphate compound present within the crystal layer.

In the low energy spectral window the set of four peaks between 900 and 1200 cm^{-1} are particularly diagnostic. The tall, sharp peak near 1000 cm^{-1} and the three other small peaks with characteristic relative intensities and locations in this region can be

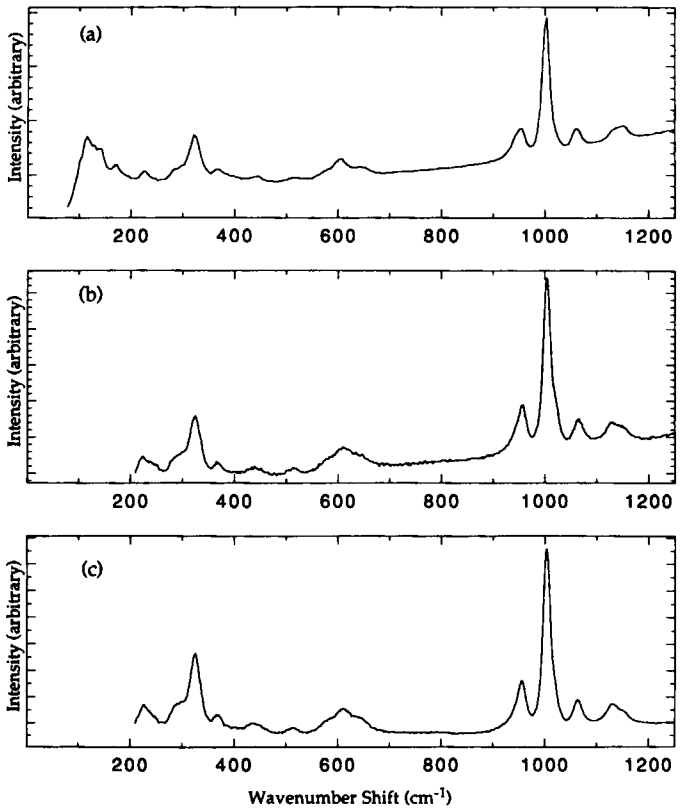

Figure 1 Representative Raman spectra used to identify surface crystallites. Spectrum (a) is from $Zn_3(PO_4)_2 \cdot 2H_2O$, zinc phosphate dihydrate. Spectrum (b) is from a zinc phosphate film grown without PAA. Spectrum (c) is from a modified film with 2% PAA in the solution bath.

Table I Frequencies of Selected Peaks With Mode Assignments

Raman Spectrum			
(a) (Reference)	(b) (Unmodified Film)	(c) (Modified Film)	Mode Assignment
225	225	225	Zn—O stretch
325	325	325	O—P—O sym. bend
605	610	610	O—P—O asym. bend
955	955	952	PO_4^{3-} stretch
1005	1005	1000	PO_4^{3-} stretch
1060	1060	1062	PO_4^{3-} stretch
1135/1150	1125/1150	1135/1150	PO_4^{3-} stretch

Raman spectra (a), (b), and (c) as shown in Figure 1. The reference is zinc phosphate dihydrate, $Zn_3(PO_4)_2 \cdot 2H_2O$. The modified film was grown in a solution bath containing 2% PAA. The peak locations are given in units of cm^{-1}.

recognized easily, as shown in Figure 1. Spectrum (a) is from $Zn_3(PO_4)_2 \cdot 2H_2O$, zinc phosphate dihydrate, as received from Alfa Products. Spectrum (b) is from a zinc phosphate film grown with no PAA in the solution bath. Spectrum (c) is from a modified film with 2% PAA in the solution bath. For comparison, Table I lists several Raman peak locations in cm^{-1} with mode assignments.[5] The peak locations and intensities match well for all three spectra, demonstrating the composition of both the modified or unmodified films to be a zinc phosphate. Subtle differences in the spectra are easily accounted for by considering different orientations of the zinc phosphate crystals or other optical effects. The small differences evidenced in the spectra are grossly smaller than would be present if the stoichiometry or crystal structure of the films were different from the standard zinc phosphate dihydrate. Most of the unlisted peaks from spectra (a), (b), and (c) in Figure 1 are associated with various O—H motions.

The dihydrate is characterized by a peak near 3400 cm^{-1}. A small shoulder near 3550 cm^{-1} was seen in some samples, which appears to be associated with excess moisture. This small shoulder is more pronounced for samples with higher amounts of PAA, and baking samples without PAA at 150°C tended to eliminate the shoulder entirely. Figure 2 shows two spectra taken on a sample without PAA. Spectrum (a) was before baking; spectrum (b) after baking at 150°C for 15 min. Baking did not change to any appreciable extent the Raman signature associated with the phosphate groups below 1200 cm^{-1}.

With Raman, two different investigative methods were carried out in an effort to detect the presence of a layer, or layers, other than zinc phosphate dihydrate. First, the exterior film was carefully removed mechanically with a sharp blade and Raman spectra obtained as a function of depth. All spectra showed zinc phosphate dihydrate until the steel substrate was reached. Second, very thin films were grown by removing the steel substrates early in the growth process. The first spectral signatures to appear were those for zinc phosphate dihydrate, which could be detected after approximately 1 min of film growth. Spectral signatures for other films were not seen using Raman.

Raman studies of our first samples of zinc phosphate films on steel gave no evidence for a multilayer model for the coating as discussed by previous workers; however, we cannot rule out the possibility of the existence of very thin inner layers near the steel surface, especially if they are very poorly ordered. Based on the earlier work[2,3] it is reasonable to expect $Fe(PO_4)_2$ and/or $Zn_2Fe(PO_4)_2 \cdot nH_2O$ near the steel surface.

However, with micro-Raman we were able find evidence for two other species on the surface of films modified with PAA. One species was conjectured to be some form of hydrated iron oxide or iron phosphate. The source of these spectra was an inclusion, somewhat transparent, but brown tainted. Figure 3 shows two micro-Raman spectra obtained with a one-micron diameter spot size from a modified film with 1% PAA in the solution bath. Spectrum (a) is from one of the inclusions. Spectrum (b), also labeled "superposition," is not, however, a simple addition of two individual spectra. Rather, it is the optical signal from a single micro-Raman spectrum of the surface. It simultaneously picks up a signature from both a zinc phosphate dihydrate crystallite and

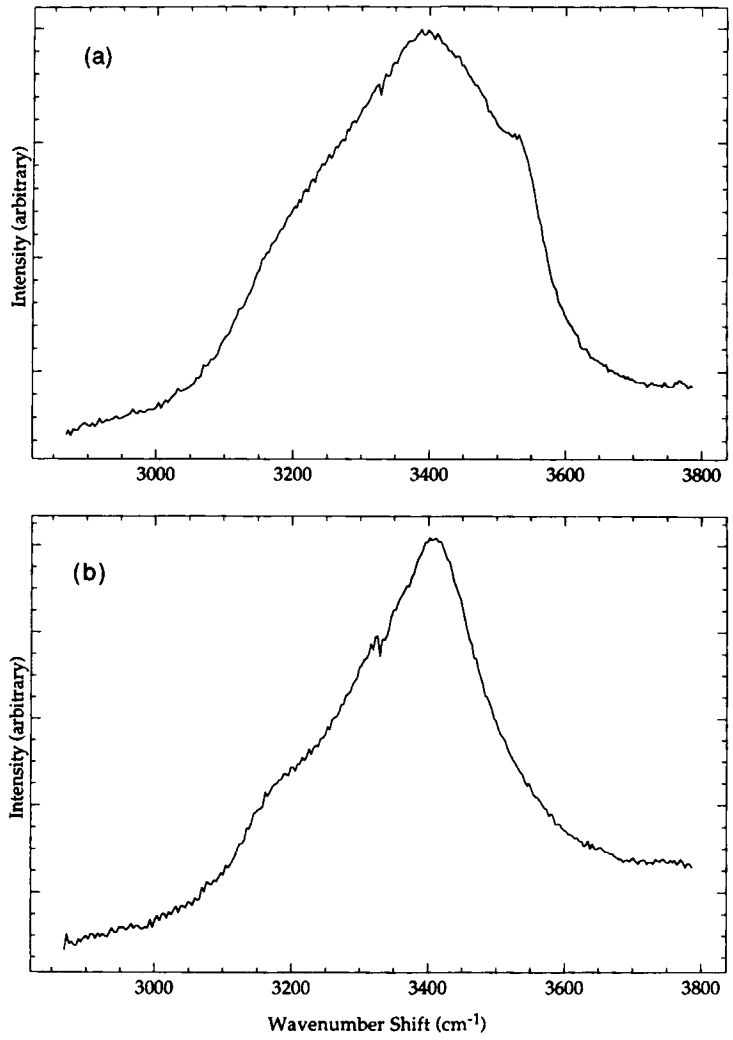

Figure 2 Two Raman spectra taken on a zinc phosphate sample without PAA. Spectrum (a) was before baking; spectrum (b) after baking at 150°C for 15 min. The structure near 3300 cm^{-1}, more obvious in spectrum (b), is an artifact of the detector.

an inclusion. The inclusion shows a strong Raman peak near 700 cm^{-1}. To identify by comparison with known spectra, Raman spectra were measured for Fe_3O_4 and for Fe_2O_3. The Fe_3O_4 showed a very strong Raman peak just below 700 cm^{-1}. The Fe_2O_3 showed a strong Raman peak near 600 cm^{-1}. The close proximity of peaks in these two prevalent iron oxides to the peak of the inclusion suggests the inclusion may contain a hydrated iron oxide. In the surrounding region the spectra were similar to those shown in Figure 2.

The other species detected by micro-Raman that were obtained from inclusions on the surface of modified films were clear and more island-like than those discussed above. Figure 4 shows the micro-Raman spectra for one of these inclusions from a modified film with 1% PAA in the solution bath. It shows a very strong peak near 2900 cm^{-1}. A peak just below 3000 cm^{-1} would correspond to a C—H stretch for aliphatic bonds. The peak near 2900 cm^{-1} is clear evidence of C—H stretch modes with aliphatic character, undoubtably from molecular segments associated with the PAA.

Although some Raman spectra showed some evidence of a broad, very weak peak in the vicinity of 2900 cm^{-1}, in general the size and nature of this peak in the Raman data were not sufficiently strong and consistent to conclude that PAA or its deriva-

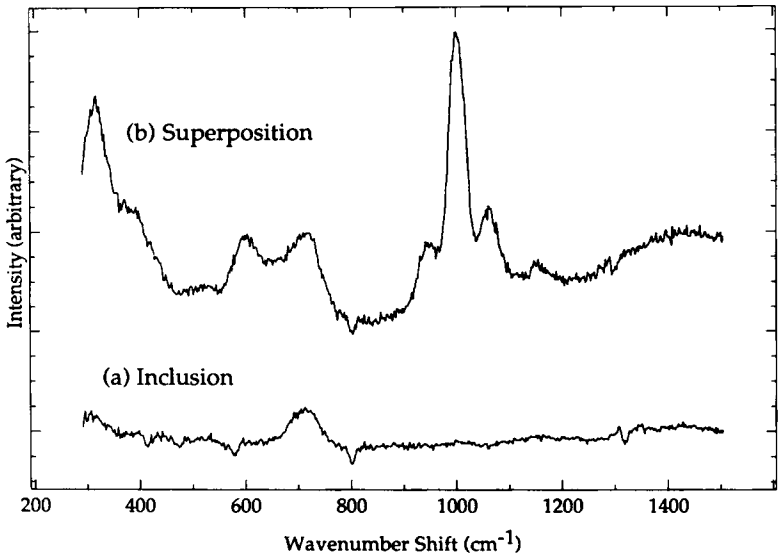

Figure 3 Two micro-Raman spectra from a zinc phosphate film modified with 1% PAA in the solution bath. Spectrum (a) is from one of the inclusions that was fairly transparent to the eye, yet with some brownish color apparent. Spectrum (b), also labeled "superposition," is the combined optical signal from a zinc phosphate dihydrate crystallite and an inclusion.

tives were being detected on the crystallite surfaces investigated, apart from the inclusions. The spectral features were quite weak compared to those from the zinc phosphate dihydrate and from the much larger peak near 3400 cm^{-1} associated with the O—H stretch from waters of hydration.

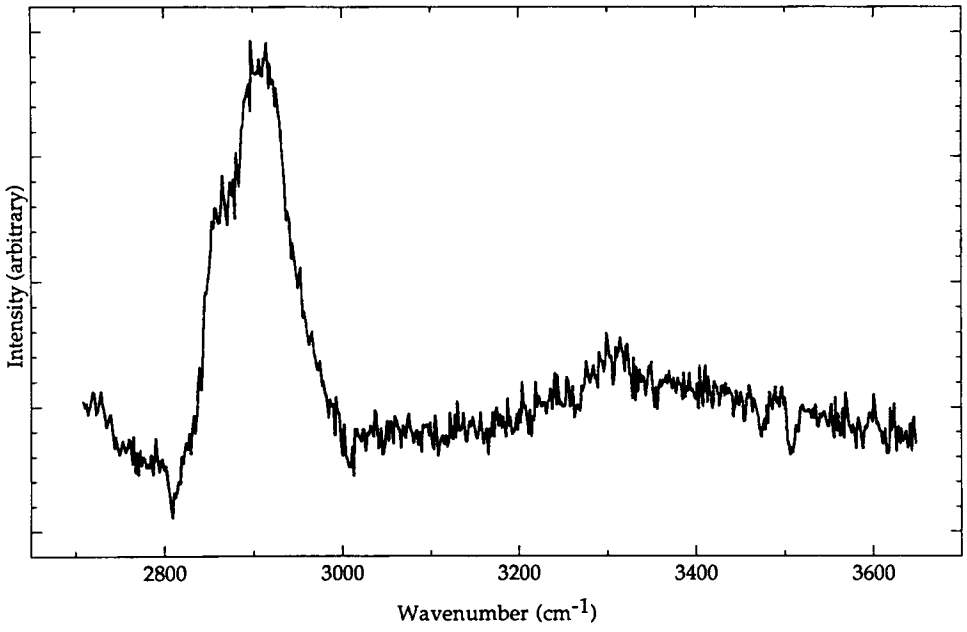

Figure 4 Micro-Raman spectra from a zinc phosphate film modified with 1% PAA in the solution bath showing a spectrum for one of the clear and more island-like inclusions than those for Figure 3. The peak near 2900 cm^{-1} is associated with C—H stretch modes.

FT-IR Spectroscopy

FT-IR spectra from the surface of PAA-modified films showed no evidence for organic groups. A variable angle reflection attachment from Harrick Scientific Corp. was used to measure surface spectra. The surfaces were rough, and the high degree of scattering caused the spectra to be quite noisy for the films investigated.

Atomic Force Microscopy

AFM images showed a number of interesting structures and features. All AFM images were taken on relatively flat "plateaus" associated with individual crystallite faces oriented more or less parallel to the steel substrate surface. While differences between the unmodified and the PAA-modified films could be observed, the general morphologies of the two types of films are similar. The significant features imaged were long striations, with a cross-striation pattern. Some differences were observed that may be associated with the addition of PAA to the phosphating bath.

AFM images obtained with the NanoScope II in the contact mode on unmodified films are shown in surface view in the four half-tones labeled Figure 5(a)–(d). Figure 5(a) is a 2 × 2 μm sub-image, taken from a 5 × 5 μm scan. Note that the scale dimension perpendicular to the surface is considerably smaller than the dimensions along the surface in all AFM scans shown. Long striations are characteristic of the surface morphologies of both modified and unmodified films, with characteristic widths ranging from less than 100 nm to about 500 nm. Figure 5(a) shows these major striations as well

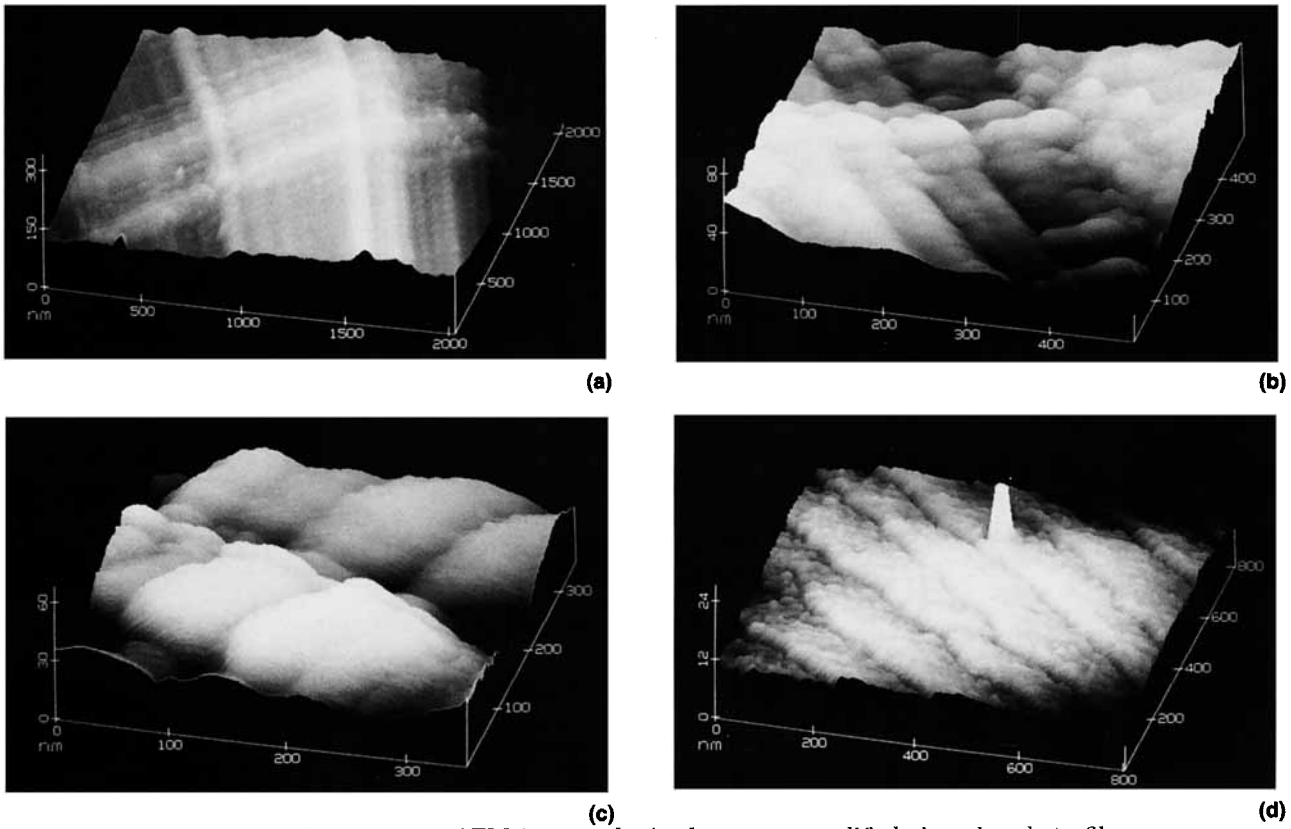

Figure 5 Four contact AFM images obtained on an unmodified zinc phosphate film taken with a Nanoscope II. Surface views are shown. Image (a) is a 2 × 2 μm subimage, taken from a 5 × 5 μm scan. Major striations as well as smaller striation-like features perpendicular to the major ones are prevalent. Note the sharp protrusions. Image (b) is a 500 × 500 nm scan taken in the neighborhood of the scan for image (a). It reveals in greater detail the small structure perpendicular to the main striations. Image (c), 350 × 350 nm, shows a close-up of a "cross" in images (a) and (b). Image (d) is a 1 × 1 μm scan from a region that is extremely flat. A close-up of one of the sharp protrusion can be seen in the upper central portion of the scan.

as smaller striation-like features perpendicular to the major ones. Some of the features appear quite sharp and angular, with several columnar-shaped protrusions evident. Figure 5(b) is a 500 × 500 nm scan taken in the neighborhood of scan for Figure 5(a). It reveals in greater detail the small structure perpendicular to the main striations. A close-up of a "cross" is shown in the 350 × 350 nm scan in Figure 5(c). Figure 5(d) is a 1 × 1 μm scan from an extremely flat region; the scale in the direction perpendicular to the surface is only a few nanometers. One of the sharp protrusions can be seen in the upper central portion of the scan.

Similarly, AFM images obtained with a Nanoscope II on a film modified with 5% PAA in the solution bath are shown in surface view in Figure 6(a)–(d). Figure 6(a) is a 1.5 × 1.5 μm scan illustrating the striated pattern prevalent on this sample. The characteristic widths of the striations varied considerably in the modified film also. Figure 6(b) is a 500 × 500 nm scan with more narrow striations than in Figure 6(a). The line pattern for the striations in the modified film crystallites tended to be wavier than those investigated in the unmodified films, with fewer sharp features. This pattern of less well-defined and less straight boundaries for striations in the modified films was often observed; we are not sure how this property might be associated with the possible presence of organic segments originating with PAA in the phosphating bath. Figure 6(c) is a 500 × 500 nm scan in a different region. Figure 6(d) is a smaller scan, 200 × 200 nm, in the same region as Figure 6(c).

AFM images obtained with the Nanoscope III on an unmodified film are shown in the top view in Figure 7. The modified film was grown in a solution bath containing 5% PAA. Figure 7(a) is a 2 × 2 μm image of the unmodified film using contact AFM. It is similar to the contact AFM taken with the Nanoscope II except for the presence of the pyramidal-

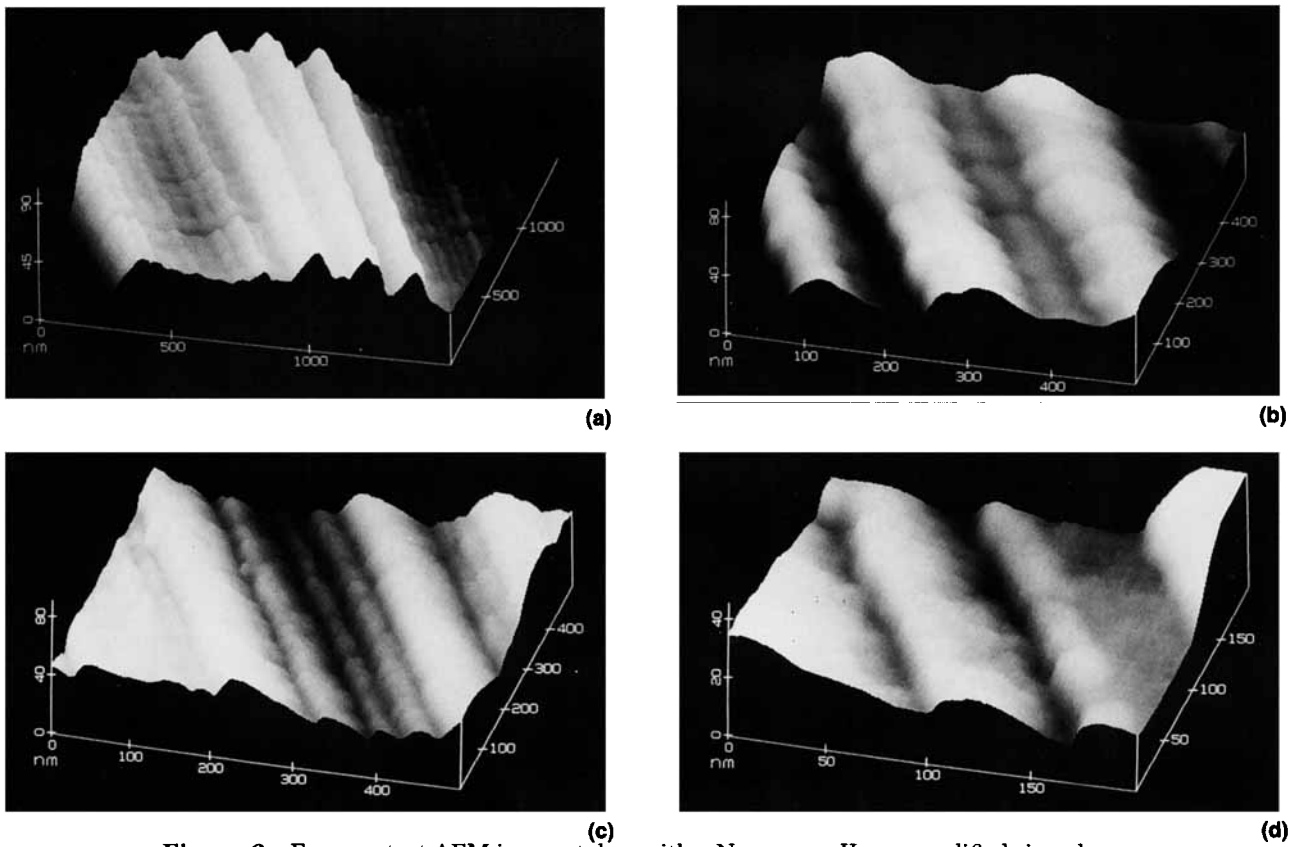

Figure 6 Four contact AFM images taken with a Nanoscope II on a modified zinc phosphate film grown with 5% PAA in the solution bath. Surface views are shown. Image (a) is a 1.5 × 1.5 μm scan illustrating the striated pattern prevalent on this sample. Image (b) is a 500 × 500 nm scan with more narrow striations than in image (a). Image (c) is a 500 × 500 nm scan in a different region. Image (d) is a smaller scan, 200 × 200 nm, in the same region as image (c).

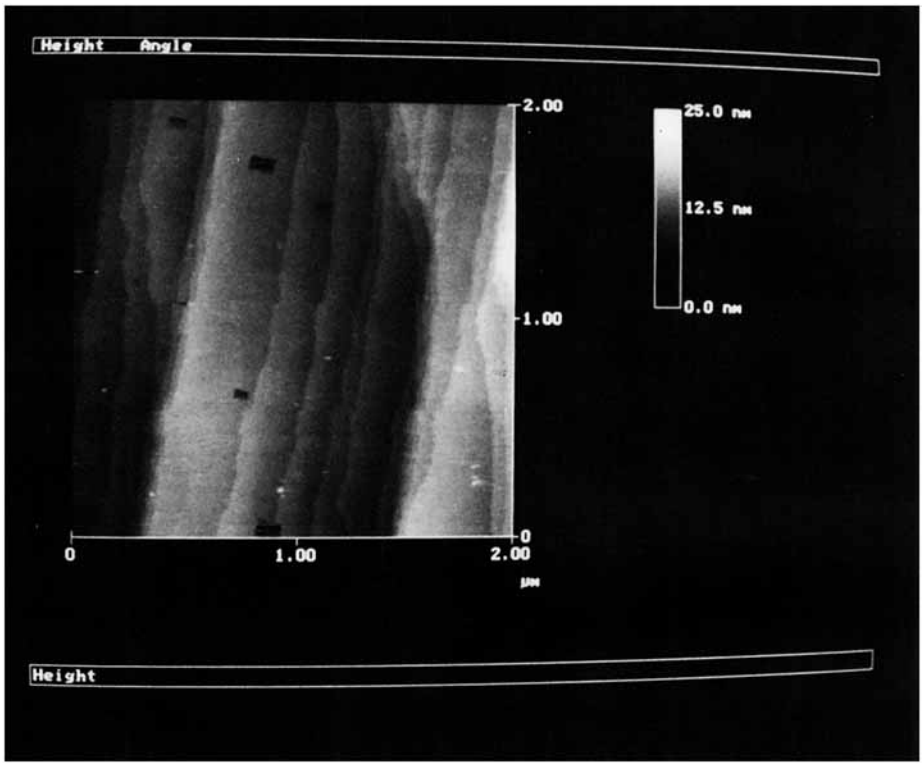

(a)

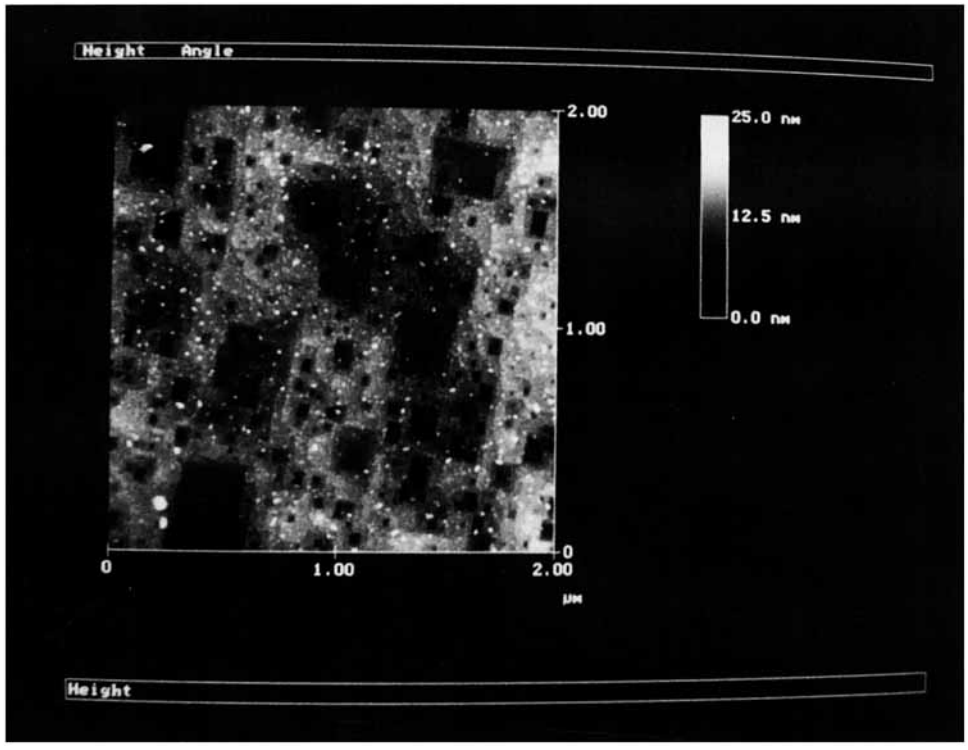

(b)

Figure 7 Contact and tapping mode AFM images taken with a Nanoscope III on an unmodified zinc phosphate film and on a modified film. The modified film was grown in a solution bath containing 5% PAA. Top views are shown in all four images. Image (a) is a 2×2 μm scan of the unmodified film using contact AFM. Image (b) is a 2×2 μm scan of the modified film using contact AFM. The surface number density of pits is greater for the modified film than for the unmodified film shown in (a). Image (c) is a 125×125 nm scan of the modified film using tapping AFM. The resolution is higher than could be obtained using Nanoscope III contact AFM. (d) is a 500×500 nm scan of the modified film using noncontact AFM. The surface features appear similar to those in (b), but at higher resolution.

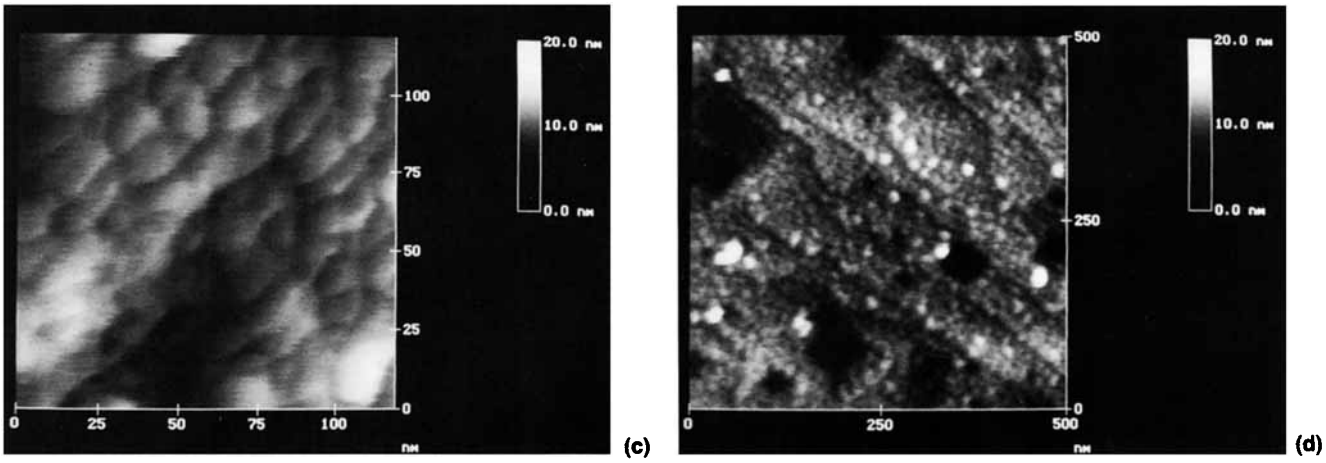

Figure 7 *(Continued from the previous page)*

shaped pits. Figure 7(b) is a 2 × 2 μm image of the modified film using contact AFM. The surface number density of pits is ostensibly greater for the modified film than for the unmodified film shown in Figure 7(a). Figure 7(c) is a 125 × 125 nm image of the modified film using tapping-mode AFM. The surface features are similar to those obtained with contact AFM using the Nanoscope II, but the resolution is higher. Figure 7(d) is a 500 × 500 nm image of the modified film using tapping mode AFM. The surface features are similar to those in Figure 7(b), except at higher resolution.

A large number of pyramidal-shaped pits in addition to the striation patterns were observed in AFM images taken with the Nanoscope III, for both contact and tapping modes. For the areas scanned, the pyramidal-shaped depressions were much more prevalent on the PAA-modified sample than on the unmodified sample. The Nanoscope II images showed far fewer depressions and were without a regularized shape. The orientation of pyramidal edges was not fixed along the direction of scanning, indicating the pits were not tip artifacts. On any given scan, however, the orientations of pit edges were in registry with one another, which would not be unexpected for defects associated with a common aspect of crystalline growth.

Thus, one difference between AFM images taken with the Nanoscope II and the Nanoscope III was that those taken with the Nanoscope III revealed pyramidal-shaped pits on both modified and unmodified films. Individual differences in tip shape—sharper ones were use on the Nanoscope III than on the Nanoscope II—may be an important parameter in explaining the fact that pits were detected in images taken with the Nanoscope III but not detected for images taken with the Nanoscope II system. However, it would seem that the pyramidal-shaped pits were too large to be explained solely by differences in tips. The Nanoscope III images were taken after the Nanoscope II images were obtained, so it is possible that the surface had suffered some corrosion causing etch pits. Also, it is possible that different crystal planes were being imaged by the Nanoscope III and the Nanoscope II, and that the different crystal planes have different growth mechanisms, causing some to be flat and some pitted. This latter phenomenon has been observed on a number of natural crystals.

The surfaces did appear rough. The standard deviations for both unmodified and PAA-modified surfaces were typically in the range of 10–20% of the surface height range.

Atomic resolution AFM images could not be obtained. The AFM images shown in Figures 5 and 6 were taken with a scan head with a 15 × 15 μm maximum scan size. A second AFM head with a smaller range, 0.8 × 0.8 μm, was also used. This smaller scan head is capable of higher resolution, primarily due to its greater mechanical stability, but images recorded using the smaller head were no clearer. On suitable samples either of these heads are capable of resolution approaching atomic scale. Thus, the inability to record higher resolution images suggests the resolution obtained was limited by subtleties associated with interactions of the tip with the sample surface. Possibilities include elastic deformation of the surface by the probing tip, electrostatic charging due to the contact of the tip with the surface, surface debris such as molecular segments

from the PAA, or capillary condensation of water in the constriction formed by the tip and sample surface.

Tapping mode AFM gave higher resolution than contact AFM. When using the tapping mode AFM on a PAA-modified film, the system was able to image 10–20-nm surface features. Features this small could not be imaged with contact AFM. A possible explanation for the difference in resolution is that the modified surface may have soft or sticky features, and these features were being distorted by the tip when using contact AFM.

CONCLUSIONS

The preponderance of crystallites on the surface of both the unmodified and PAA-modified surfaces were zinc phosphate dihydrate as evident from the Raman and micro-Raman spectra.

The surfaces of the individual crystallites investigated were rough and nonperiodic. AFM was successful in obtaining surface morphologies of single crystallite surfaces for both unmodified and modified films. The AFM images for the two surfaces show qualitative differences in morphology, although both are characterized by long striations with widths from less than 100 nm up to several 100 nm. Rectangular-shaped pits were quite apparent in AFM images taken with the Nanoscope III system. For the surface areas investigated, the surface density of pits was higher for the modified films than for unmodified films. The common orientation of pit edges within a scan on a crystallite suggests the mechanism of pit formation is intimately related to the mechanisms of crystal growth and structure.

Specific organic molecular segments could not be identified in the AFM images, even though the apparent resolution appeared sufficient to allow large entanglements to be imaged. Higher resolution could be obtained with tapping mode AFM than with contact AFM when investigating modified films. These differences can reasonably be ascribed to the different growth conditions in the phosphating baths, that is, with and without PAA. The presence of the PAA would increase the number of nucleation sites and thereby increase the number of defect sites, such as pits. FT-IR results were not helpful in identifying PAA on the surface.

It is reasonable for SEM micrographs to show major changes in surface structure; whereas, the AFM may not, since the scales are quite different. The SEM images are at lower magnification and show agglomerations of crystallites, the size and matrix of which change with the addition of PAA. The AFM images are from the surface of an individual crystallite, which may not change as dramatically as crystallite size with the addition of PAA.

In summary, the spectroscopic and microscopic evidence for the presence of molecular segments from the PAA on or in the crystallites for the modified films is weak at best. One possibility is that PAA segments preferentially adsorb on crystal faces other than the dominant plane, which is in the plane of the sample surface. It is quite possible that the PAA has a stronger affinity for the side facets of the crystallites. Thin (i.e., a molecule or two thick) but more or less complete coverage by PAA there would be consistent with the a very weak Raman and IR signature, but could easily influence the growth of the crystallites and have the pronounced adhesion improvements for topcoatings. It is also possible that the water rinsing during film preparation could wash much of the water-soluble polymer from the external crystal surfaces.

This work was supported in part by the U.S. Army Research Office (Research Triangle Park, NC) under Contract No. DAAL03-89-K-0084 and DAAL03-92-G-0372, and the University of Missouri, Grant No. 90-WS-015.

REFERENCES

1. E. L. Ghali and J. J. Potvin, *Corrosion Sci.*, **12,** 583 (1972).
2. T. Sugama, L. E. Kukacka, N. Carciello, and J. B. Warren, *J. Appl. Polym. Sci.*, **30,** 4357 (1985).
3. T. Sugama, L. E. Kukacka, N. Carciello, and J. B. Warren, *J. Appl. Polym. Sci.*, **32,** 3469 (1986).
4. T. Sugama, Technology Transfer Workshop for Zinc Phosphate Coating R&D, U.S. Army Research Office, Research Triangle Park, NC, June 23, 1987.
5. L. C. Thomas and R. A. Chittenden, *Spectrochimica Acta,* **20,** 489 (1964).

Received November 13, 1992
Accepted March 14, 1993